DETECTION AND DIAGNOSIS OF REPETITIVE SURFACE DEFECTS FOR HOT ROLLING PROCESSES

Qiang Li and Jionghua (Judy) Jin
Department of Industrial and Operations Engineering
University of Michigan
Ann Arbor, Michigan

Tzyy-Shuh Chang
OG Technologies, Inc.
Ann Arbor, Michigan

KEYWORDS

Hot rolling process, image processing, repetitive pattern, surface defect, monitoring and diagnosis.

ABSTRACT

This paper presents a new technique for automatically detecting and diagnosing the repetitive surface defects in hot rolling. In the paper, surface image data of the hot rolled bars is online collected using advanced image sensors, and an automatic defect detection algorithm is developed for identifying the roll-induced repetitive surface defects by integrating the Canny detector and the Hough transform. After detecting the repetitive surface defects, an estimation algorithm is further used for robustly estimating the repetitive periodicity. Furthermore, a knowledge-based root-cause diagnosis approach is proposed for identifying the stand with the broken roll failure based on the estimated period of defect patterns. A real-world case study is provided in the paper to demonstrate and validate the proposed method.

INTRODUCTION

Imaging-based automatic online inspection of surface defects has raised increasing research interests in recent years for the process control in hot rolling. Some fast algorithms have been previously developed for online defect detection and identification of individual defects (Jia, 2004; Li et al., 2007). However, previous research has mainly focused on detecting “individual” defects with the specific shape pattern, such as seams. Few were found on identifying “group” defects with repetitive patterns. It is known when a roll failure happens, a group of the repetitive defects will be generated on product surfaces, and thus leads to severe product scrap. In another aspect, the periodicity of the repetitive defect patterns is closely related to the specific stand where the roll failure occurs, and provides the physical mechanism to identify the root causes of the repetitive defects for a quick process correction decision. Therefore, it is highly demanded in hot rolling manufacturing industry to develop an effective monitoring and diagnostic system that can not only quickly detect surface defects, but also identify the repetitive nature of the detections for root cause diagnosis.

The objective of this paper is to develop an effective monitoring and diagnostic method for quickly detecting and diagnosing repetitive surface defects caused by roll failure. The remainder of this paper is organized as follows. After this introduction section, a new detection and estimation algorithm will be introduced for identifying repetitive surface defects and estimating the period of the repetitive defect patterns. Afterward, an engineering knowledge based root-cause diagnosis approach is proposed for identifying the specific stand with the roll failure. A real-world case study is then provided to demonstrate and validate the proposed method. Finally, a summary and some future work are given.

DETECTION OF REPETITIVE DEFECT PATTERN

The first step of this research is to automatically detect the repetitive defect pattern. FIGURE 1 describes the major procedures proposed in the paper.

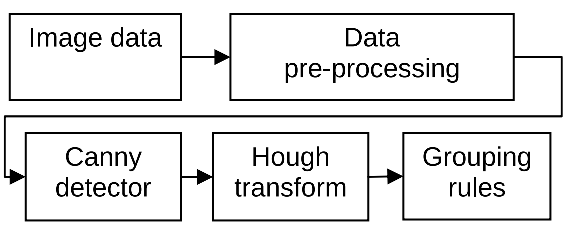

FIGURE 1. DETECTION METHOD PROCEDURES.

First of all, the image data will go through some necessary image preprocessing steps like image cutting and vibration pattern removal. The next important step is to find the members of the repetitive pattern based on the Canny detector and the Hough transform by taking advantage of the common properties in the shape of the repetitive pattern members. Finally the detected defects will be grouped and be indentified if they satisfy the rules for checking the repetitive patterns. In the following subsections, the major steps for developing the detection and grouping rules will be discussed.

<u>Detection of Individual Defect Members</u>

For detecting the repetitive defect patterns, the first step is to find all the candidate members of the suspected defects in the images collected by the on-line imaging system. After that, we can use grouping rules to check whether these defect members have a potential repetitive pattern.

To understand the unique properties of the repetitive defect pattern, it is necessary to understand the mechanism of online imaging system from where the product surface images are obtained. The core sensor is capable of capturing the objects' surface condition at a high temperature environment. An example of image with repetitive defects pattern is shown in FIGURE 2.

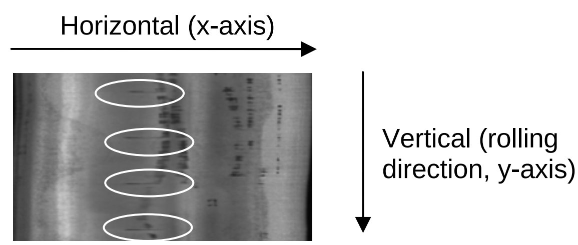

FIGURE 2. A REPETITIVE PATTERN EXAMPLE.

In practice, 80-90% of defects induced by roll failures exhibit marks as thin horizontal lines. Therefore, based on the shape characteristic of the repetitive defects, the objective of detecting individual suspect is transformed to detecting the vertical line-shape defects. Starting from the idea of taking advantage of the shape properties, the line detection method is developed by integrating the Hough transform (Ballard, 1981) and Canny edge detector (Canny, 1986). Comparing to the detection of defects of a general shape, the proposed detection algorithm requires much less computational effort (Illingworth, 1988) and thus is feasible to be implemented for the online purpose. Moreover, the falsely detected defects due to complex background noises are also significantly reduced.

<u>Canny Detector.</u> The first step is to detect the edge points by using appropriated edge detector (Gonzalez, 2007). The Canny detector is selected because it is an optimal edge detector, which has a low error rate and the good edge point localization capability to generate thin edges with respect to other derivative methods (Sobel, 1970; Marr and Hildreth, 1980). The implementation of canny detector is given as follows:

The image object can be denoted as $f(x,y)$ as shown in FIGURE 3(a), where the repetitive defects are marked. x and y are the coordinates of image pixels. The image $f(x,y)$ will be firstly smoothed by convolving a 2-dimensional Gaussian function in order to avoid the effect from noisy pixels. After de-noising, the image is denoted as $I(x,y)$, which are gradient magnitudes having ridge thinning. To find the real edge points in $I(x,y)$, the double thresholding strategy is used as follows based on two defined thresholds: i.e., the low threshold T_L and the high threshold T_H.

If the points satisfy

$$I(x,y) \geq T_H , \quad (1)$$

these points are called "strong" edge points and identified as edge points directly. If the points satisfy

$$T_L \leq I(x,y) \leq T_H , \quad (2)$$

these points are called "weak" edge points. If the weak points are the neighbors of the strong points, they are identified as the edge points; otherwise they will be ignored. If the gradient value range is scaled to 0 and 1, the high threshold T_H can be selected from 0.01 ~ 0.3 based on the image conditions from different plants. The low threshold T_L is suggested to be 30% ~ 50% of T_H.

Finally all the strong points and the corresponding neighboring weak points will be detected as edge pixels. The output of the Canny detector, as shown in FIGURE 3(b), is a binary image $f_b(x,y)$, i.e.,

$$f_b(x,y) = \begin{cases} 1 & (x,y) \text{ is the edge point;} \\ 0 & \text{otherwise} \end{cases} \quad (3)$$

Hough Transform. After using the Canny edge detector, the original image is transformed to a binary image. On the binary image, the Hough transform (Ballard, 1981) is used to identify those defects having a line shape and consider them as suspect members of the repetitive defect patterns. In the Hough transform, the following representation of a line is used:

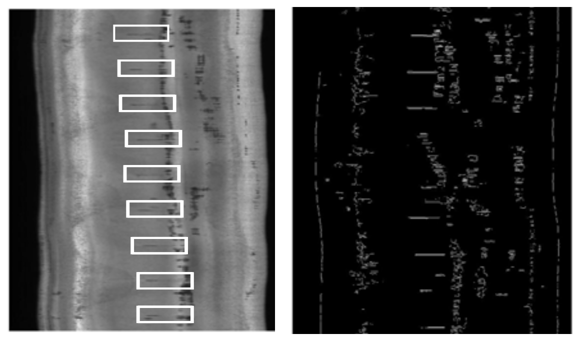

FIGURE 3. (a) THE ORIGINAL IMAGE WITH REPETITIVE PATTERN; (b) THE BINARY IMAGE OBTAINED AFTER USING CANNY DETECTOR.

$$x \cos\theta + y \sin\theta = \rho \quad (4)$$

The implementation of the Hough transform is given as follows. Firstly, divide the values of ρ and θ with equal steps within the parameter ranges of $[\rho_{\min}, \rho_{\max}]$ and $[\theta_{\min}, \theta_{\max}]$. For θ, the range of $-5^\circ \leq \theta \leq 5^\circ$ is used to identify horizontal lines. Let I and J be the numbers of subdivisions for θ and ρ, respectively. Given an edge point (x,y) found in the Canny detector, for each θ_i ($i = 1,\ldots,I$), calculate the corresponding value of ρ using equation (4). The calculated ρ value is approximated to the closest subdivision value ρ_j, ($j = 1\ldots J$). Denote $A(i,j)$ as the accumulator value corresponding to the accumulator cell (ρ_j , θ_i). When a pair of (ρ_j , θ_i) is found using the searching method discussed above, $A(i,j) = A(i,j) + 1$. This step is iterated until all edge points have been checked. Afterwards, find all the accumulator cells that satisfy:

$$A(i,j) \geq T_a \quad (5)$$

where T_a is the threshold to measure points' concentration on a line. The lines corresponding to the found accumulator cells are detected, as shown in FIGURE 4(a).

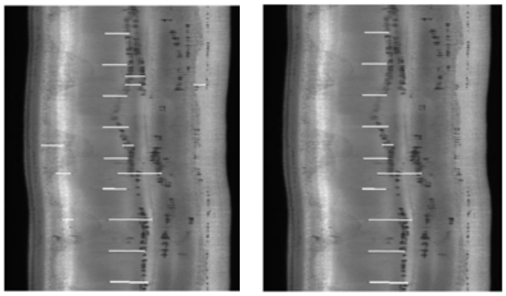

FIGURE 4. (a) THE DETECTION RESULT AFTER HOUGH TRANSFORM; (b) THE FINAL DETECTION RESULT AFTER USING TWO RULES.

Two Rules for Identifying Repetitive Patterns

Two rules, which are called grouping and identification rules, will be presented in this section, in which the grouping rule as Rule 1 is used to remove the falsely detected defect members based on the locations of defect lines; and the identification rule as Rule 2 is used to further reduce false alarms based on the lengths of defect lines and to check whether a repetitive pattern is existing. The flowchart of these two rules is illustrated in FIGURE 5.

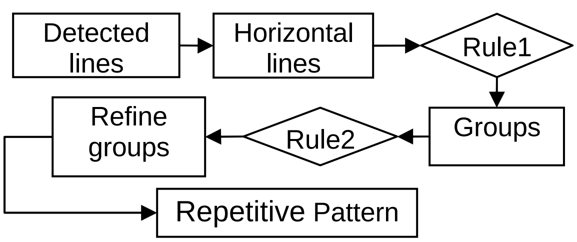

FIGURE 5. PROCEDURES FOR IDENTIFYING REPETITIVE DEFECT PATTERNS.

Rule 1 is used to group the horizontal lines based on their locations along the horizontal direction because repetitive defect members should correspond to the same failed roll, which generates the repetitive defects having the overlapping location along the horizontal direction. For this purpose, each line is represented as a location vector $\mathrm{l} = (l_{L,} \ l_R)^T$, where l_L and l_R are the x-axis (horizontal) coordinate corresponding to the left point and right point of the line, respectively. Before using Rule 1, all horizontal lines are sorted by l_L in the ascending order as $\mathrm{l}^{(1)}, \mathrm{l}^{(2)}, \ldots, \mathrm{l}^{(m)}, \ldots \mathrm{l}^{M}$. Beginning from the most left one (the one with the smallest x-coordinate $\mathrm{l}^{(1)}$), if the location vector of he selected line $\mathrm{l}^{(m)}$ satisfies

$$l_R^{(m-1)} - l_L^{(m)} > T_l \,, \qquad (6)$$

$\mathrm{l}^{(m)}$ will be grouped into the previous group with $\mathrm{l}^{(m-1)}$; otherwise $\mathrm{l}^{(m)}$ will be put into a new group. Rule 1 will be iterated until all the lines are checked. T_l is the threshold, which is used to measure the overlapping length of two lines along the horizontal direction.

Rule 2 is used to remove the abnormal lines that have either too large or too small lengths by comparing the lines within the same group. For each grouped lines, the mean $\bar{u}$ and the standard deviation std_u of the line lengths are calculated. The line whose lengths are out of the interval $[\bar{u} - 3std_u, \bar{u} + 3std_u]$ will be removed. After using Rule 2, if there are more than three defect lines are identified in the group, that group will be considered as the repetitive pattern group, which are shown as FIGURE 4(b).

ESTIMATION OF DEFTECT PERIODICITY FOR ROOT CAUSE DIAGNOSIS

Diagnosis Model

As long as the repetitive defect patterns are detected, the next question will be how to identify the specific stand with the failed roll that causes the repetitive pattern of defects. For this diagnosis purpose, it is essential to introduce the concept elongation coefficient used in the rolling processes (Wusatowski, 1969).

The elongation coefficient for a rolling mill is defined as:

$$e = \frac{l}{L} = \frac{A}{a} \qquad (7)$$

where L is the length of the billet before passing the mill; l is the length of the billet after passing the mill; A is the cross-sectional area of the steel billet before passing the mill; and a is the cross-sectional area of the steel billet after passing the mill. Equation (7) holds because the volume of steel does not change after passing the mill, i.e. $la = LA$.

When a roll crack happens in the rolling mill i, it will generate repetitive defect pattern on the final product surface. The ideal periodicity of the repetitive pattern for each roller is related to the roller's diameter and process operation parameters, which can be calculated based on the formula shown in reference (Wusatowski, 1969):

$$P_i = C_i \prod_{j=i+1}^{n} e_j \quad (8)$$

where P_i is the ideal periodicity of repetitive defects by stand i on the final product; C_i is the circumstance of roll i. All the parameters for calculating P_i can be obtained from the production plant. During the production, after obtaining the estimated periodicity based on the detected repetitive defect images, the cracked roller stand position will be identified based on the match between the estimated periodicity and the ideal periodicity range. Since P_i is pre-determined based on the rolling pass design knowledge and P_i is different for each stand, the key factor that affects diagnosis accuracy will be the estimation error of the defect periodicity $\hat{p}$.

Estimation of Defects' Periodicity

Each defect position along the y-axis can be consecutively encoded as one dimensional coordinate relative to the position of the first defect taken as the origin (k=0), as shown in FIGURE 6.

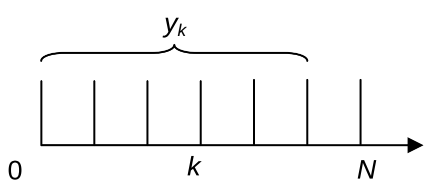

FIGURE 6. DEFECTS POSITIONS ENCODING.

For each y_k, we have the following equation in the ideal condition:

$$y_k = p \cdot k + \varepsilon_k \quad (9)$$

where $k = 0, 1, 2 \ldots N$; N is the number of intervals between defect members; y_k represents the distance of the $(k+1)^{th}$ detected defect to the origin ($k = 0$); p is the ideal periodicity of the repetitive pattern; ε_k is noises, which is assumed to be i.i.d. and follow $\varepsilon_k \sim N(0, \sigma^2)$.

Equation (9) is a simple linear regression model, which can be directly used for estimating p. However, such an estimate is very sensitive to the performance of the defect detection algorithm. For example, if a miss detection or false alarm of the defect members occurs, it will cause outliners due to the miss-match between k and y_k, thus affect the estimation accuracy of the p value.

In order to avoid accumulation errors due to the missing detections or false alarms of the defect members, Equation (9) is rewritten as follows to consider the distance interval between two consecutive defects.

$$x_k = y_k - y_{k-1} \quad (10)$$

where $k = 1, 2 \ldots N$; $y_0 = 0$. The new linear model for p estimation is

$$x_k = p + \xi_k \quad (11)$$

where $\xi_k = \varepsilon_k - \varepsilon_{k-1}$. Based on equation (11), there is only one scale parameter to be estimated, which can be considered as a special case of regression model (with only intercept). For the regression estimation problem, the Original Least Square (OLS) regression is commonly used. The OLS estimator for this simple liner model (Faraway, 2005) will be the arithmetic mean of x_k :

$$\hat{p} = \frac{\sum_{k=1}^{N} x_k}{N} \quad (12)$$

Furthermore, we can obtain that by

$$\sum_{k=1}^{N} x_k = y_N - y_0 = y_N \quad (13)$$

Therfore, equation (12) can be rewritten as

$$\hat{p} = \frac{y_N}{N} \quad (14)$$

Although such an estimator is not sensitive to the outlier of the specific interval between two consecutive defect members, it is still affected by the number of the detected defects within the measured length of the rolled products. In fact, N is affected by the miss detection rate and false alarm rate. The miss detection is basically inevitable during detection algorithm. Assume the true periodicity value to be p . If there exists a miss detection rate equal to β, which is defined as the percentage of the defect members that are not detected by the detection algorithm, the true number of the defects between y_0 and y_N generated by the rolling mill should be $\frac{N}{1-\beta}$, thus

$$\frac{y_N}{N} = \frac{p}{(1-\beta)} \quad (15)$$

Therefore, OLS will lead to an over estimation of the true periodicity. The bias can be calculated as:

$$bias(\hat{p}) = \hat{p} - p = \frac{y_N}{N} - p = \frac{\beta}{1-\beta} p \quad (16)$$

In this paper, the false positives are considered as false alarmed members of the repetitive pattern. Those false positives may be caused by other types of individual defects, roll marks, or material texture, which show the line-shape pattern similar to the repetitive pattern members. The influence of these false positives on the periodicity estimation by using OLS is discussed as follows.

Under the false alarm rate equal to α , the true number of the defects between y_0 and y_N should be $(1-\alpha)N$, thus

$$\frac{y_N}{N} = (1-\alpha)p \quad (17)$$

This will lead to an under estimation of the true periodicity. The bias under this condition will be

$$bias(\hat{p}) = \hat{p} - p = \frac{y_N}{N} - p = -\alpha p \quad (18)$$

In order to overcome such biased estimation problem, a robust estimation method based on Least Median of Squares (LMS) is used in the paper (Rousseeuw, 1984). Compared to the OLS estimator, the LMS estimator has better performance in estimator robustness (Rousseeuw, 1987).

The general LMS algorithm can be much simplified in our paper for the special estimation given in equation (12). The algorithm of the LMS estimator is applied by determining the shortest half of the samples, which is done by calculating the following differences (Rousseeuw, 1987):

$$x^{(h)} - x^{(1)}, x^{(h+1)} - x^{(2)}, \ldots, x^{(N)} - x^{(N-h+1)} \quad (19)$$

where $x^{(1)} \le \cdots \le x^{(N)}$ are the ordered observations. h is equal to $[N/2]+1$. The shortest half is the subsample which has the smallest difference calculated from equation (19) with h objects. Then, $\hat{p}$ simply equals the median of the shortest half subset:

$$\hat{p} = median(x^{h+t})_{arc\min_t (x^{(h+t)} - x^{(t)})} \quad (20)$$

Simulation Results

In this section, the performance of OLS and LMS will be compared using different sample numbers in three different conditions (with noise only, with miss detection, and with false alarms). The simulation data are generated as follows: by using equation (9), the defects with only noise are generated. The noise $\varepsilon_k \sim N(0,\sigma^2)$. According to the expected performance of the previous discussed repetitive pattern detection algorithm and the real image testing results, two worse conditions in which the miss detection rate and false alarm rate are equal to 0.2, respectively, are simulated. The estimation performance of both estimators under three different conditions: a) with only noise; b) with miss detection; and c) with false alarm are shown in FIGURE 7 and FIGURE 8 for the average and standard deviation of the estimations, respectively.

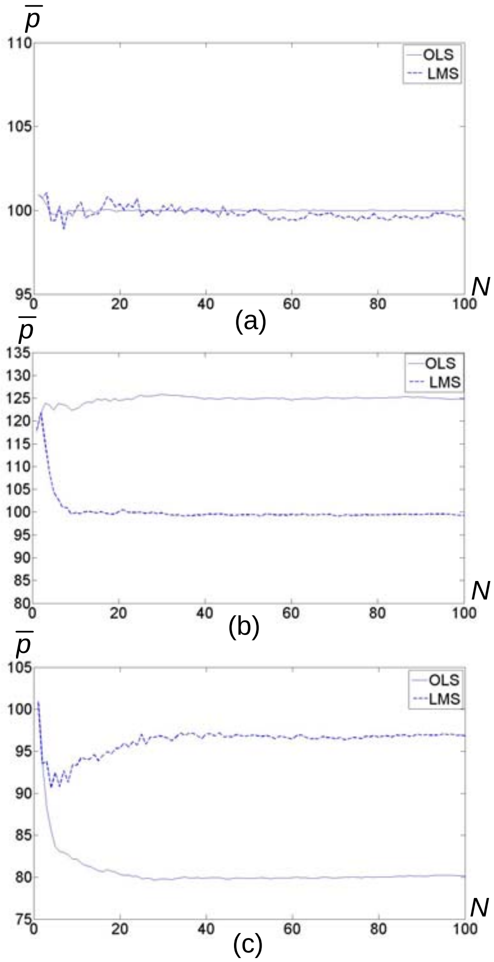

FIGURE 7. (a) AVERAGE ESTIMATIONS WITH NOISE ONLY; (b) AVERAGE ESTIMATIONS WITH MISS DETECTION; (c) AVERAGE ESTIMATIONS WITH FALSE ALARM.

In these simulations, the true value of periodicity $p_0 = 100$ and $\sigma = 0.1 \times p_0 = 10$. For each given *N* from 0~100, the performance plots of $\hat{p}$ is plotted by 100 generations in the simulations. FIGURE 7 shows the averages $\bar{p}$ given different values of *N*. It can be seen that the OLS estimator is very sensitive to the miss detection and false alarms, while the LMS estimators are nearly unbiased comparatively. In FIGURE 8 the standard deviations of the estimated periodicity values are also compared under different conditions. It shows that the false positives/ miss detection has little impact on the estimated periodicity by using the robust LMS algorithm. Therefore all detected members including tolerable false positives can be used to estimate the periodicity instead of separating all the false positives from the true defects members.

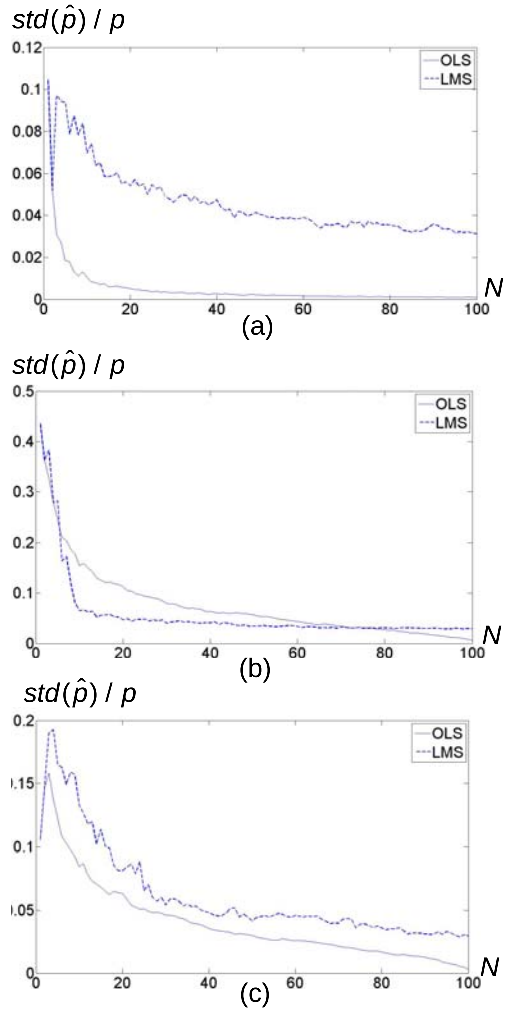

FIGURE 8. (a) STANDARD DEVIATION WITH NOISE ONLY; (b) STANDARD DEVIATION WITH MISS DETECTION; (c) STANDARD DEVIATION WITH FALSE ALARM.

CASE STUDY

In this section, the whole detection and diagnosis strategy is implemented in a real world rolling process. The products in the images are the rods with 8 mm in diameter. In the detection step, based on the proposed detection method, the repetitive pattern of the defects is detected. The detection result is shown in FIGURE 4(b).

There are 11 detected defects (i.e. 10 intervals), of which 9 are true and 2 are false alarms. The interval distances (*ID*) between these defects are calculated to be: 560, 555, 560, 330, 230, 270, 277.5, 557.5, 560, 560 mm. Therefore, the estimators of OLS and LMS can be calculated according to equation (12) and (20), respectively. The final estimated periodicities are 446 mm for OLS and 560 mm for LMS. In this case study, it has been known that the root cause is on the last second roll, which has the periodicity range [528 584] calculated based on equation (8). It is shown that LMS estimator falls into the range and gets a correct diagnosis result. The OLS cannot get the correct result because of the serious bias induced by the false alarms.

SUMMARY AND FUTURE WORK

In this paper, automatic monitoring and diagnosis of a specific repetitive pattern of surface defects in the hot rolling process is investigated. The proposed method consists of following key elements: a detection algorithm for defect image detection by integrating Canny detector and Hough Transform, two rules for identifying the repetitive patterns based on the detected defect members, a robust estimation algorithm for estimating periodicity of the repetitive defect patterns. Also, an engineering knowledge guided diagnostic approach is proposed in the paper. A real world case study is provided in the paper for demonstrating and validating of the developed method. In the future, the effort will be made on improving the detection accuracy. Furthermore, the multiple occurrences of various repetitive patterns due to multiple roll failures will also be further studied in future.

ACKNOWLEDGEMENT

This research is jointly supported by NSF DMI F0541750 and Michigan 21st Century Jobs Fund F015886. The authors would also like to thank Dr. Hongbin Jia at OG Technologies, Inc and Mr. Ran Jin at Georgia Institute of Technology for their value help on this research.

REFERENCES

Ballard, D.H. (1981). "Generalizing the Hough Transform to Detect Arbitrary Shapes." *Pattern Recognition*, Vol. 13, pp. 111-122.

Canny, J. (1986). "A Computational Approach to Edge Detection." *IEEE Transcation of Pattern Analysis and Machine Intelligence*, Vol.32, pp. 252-260.

Faraway, J.J. (2005). *Linear models with R*. CRC Press LLC., Boca Raton, Florida.

Gonzalez R.C., R.E. Woods (2007). *Digital image processing*. Pearson Education, Inc., Upper Saddle River, New Jersey.

Illingworth, J., and J. Kittler (1988). “A Survey of the Hough Transform.” *Computer Vision, Graphics, and Image Processing,* Vol. 44, pp. 87-116.

Jia, H., Y.L. Murphey, J. Shi, and T.S. Chang (2004). "An Intelligent Real-time Vision System for Surface Defect Detection." *Pattern Recognition ICPR 2004. Proceedings of the 17th International Conference on*, Vol.3, pp. 239-242.

Li, J., J. Shi, and T.S. Chang (2007). "On-Line Seam Detection in Rolling Processes Using Snake Projection and Discrete Wavelet Transform." *Journal of Manufacturing Science and Engineering*, Vol. 129, pp. 926-933.

Mallows, C.L. (1975). "Some Comments on *Cp*." *Technometrics*, Vol. 15, pp. 661-678.

Marr, D. and E. Hildreth (1980). "Theory of Edge Detection." *Proceedings of the Royal Society of London. Series B, Biological Sciences*, Vol. 207, pp. 187-217.

Rousseeuw, P.J., and A.M. Leroy (1987). *Robust Regression and Outlier Detection.* Jonh Wiley & Sons, Inc., New York.

Rousseeuw, P.J. (1984). "Least Median of Squares Regression." *Journal of the American Statistical Association*, Vol. 79, pp. 871-880.

Sobel, I.E. (1970). *Camera models and machine perception*. Stanford University, Stanford, California.

Wusatowski, Z. (1969). *Fundamentals of Rolling.* Pergamon Press, New York.